

Geophysical Research Letters®

RESEARCH LETTER

10.1029/2021GL092801

Key Points:

- This study presents first osmium isotopic composition on glacier surface impurities from the Himalaya
- Osmium isotopes and trace metal composition showed predominantly crustal sourced input
- Anthropogenic emission residues are not one of the significant drivers of glacier melting in the western Himalaya, as observed elsewhere

Supporting Information:

Supporting Information may be found in the online version of this article.

Correspondence to:

S. Nizam,
sarwar@iitk.ac.in

Citation:

Nizam, S., Sen, I. S., Shukla, T., & Selby, D. (2021). Melting of the Chhota Shigri Glacier, western Himalaya, insensitive to anthropogenic emission residues: Insights from geochemical evidence. *Geophysical Research Letters*, 48, e2021GL092801. <https://doi.org/10.1029/2021GL092801>

Received 5 FEB 2021
Accepted 10 SEP 2021

Author Contributions:

Conceptualization: Sarwar Nizam, Indra S. Sen
Data curation: Sarwar Nizam, Tanuj Shukla
Formal analysis: Sarwar Nizam, Indra S. Sen, Tanuj Shukla
Funding acquisition: Indra S. Sen
Investigation: Sarwar Nizam, David Selby
Methodology: Sarwar Nizam
Supervision: Indra S. Sen
Writing – original draft: Sarwar Nizam, Indra S. Sen, Tanuj Shukla, David Selby
Writing – review & editing: Sarwar Nizam, Indra S. Sen, Tanuj Shukla, David Selby

Melting of the Chhota Shigri Glacier, Western Himalaya, Insensitive to Anthropogenic Emission Residues: Insights From Geochemical Evidence

Sarwar Nizam¹ , Indra S. Sen¹ , Tanuj Shukla¹ , and David Selby^{2,3} 

¹Department of Earth Sciences, Indian Institute of Technology Kanpur, Kanpur, India, ²Department of Earth Sciences, University of Durham, Durham, UK, ³School of Earth Resources, State Key Laboratory of Geological Processes and Mineral Resources, China University of Geosciences, Wuhan, Hubei, China

Abstract Himalayan glaciers are invariably covered by supra-glacial debris. Of these glaciers, the Chhota Shigri Glacier (CSG) in the western Himalaya has minimal debris cover (3.4%), yet has a comparable melt rate to other Himalayan glaciers. Utilizing osmium isotopic composition, and major and trace element geochemistry of cryoconite, a dark colored aggregate of mineral and organic materials on the surface of the ablation zone of the CSG, we show that the surface of CSG is essentially free of anthropogenically emitted particles, contrary to many previous findings. Given this and the overall lack of debris, we conclude that the high melt rate of CSG is primarily related to the increase of the Earth's near-surface temperature linked directly to global warming. Therefore, the future meltwater supply for glacial-fed rivers originating from Lahaul and Spiti region would be most vulnerable for >50 million population living downstream and requires immediate attention.

Plain Language Summary Industrially derived particles are commonly deposited on Himalayan glaciers and have been proposed to be a major driver of glacier melting. Yet, the abundance of such material is highly variable across the Himalaya. The Chhota Shigri Glacier system despite having minimal debris cover and limited anthropogenic emission residues has experienced high ice volume loss since the end of the 20th century (Azam et al., 2019, <https://doi.org/10.1016/j.jhydrol.2019.04.075>). We surmise that the elevated glacial mass wastage in Lahaul Spiti valley of the western Himalaya is much likely insensitive to anthropogenically sourced pollutants but primarily climate controlled as claimed by previous studies (Azam et al., 2014, <https://doi.org/10.5194/tc-8-2195-2014>; Gantayat et al., 2017, <https://doi.org/10.1017/aog.2017.21>).

1. Introduction

Air pollution on the southern slopes of the Himalayas has reached high-altitude sparsely populated regions such as Khumbu (5,079 m a.s.l.) in Nepal (Bonasoni et al., 2010) and Hanle (4,520 m a.s.l.) in India (Babu et al., 2011). The pollutants emitted from different anthropogenic sectors in the Indo-Gangetic Plains (Saikawa et al., 2019) are transported to the high-altitude Himalaya by the southwest Indian Summer Monsoon (Cristofanelli et al., 2014; Singh et al., 2020). The presence of anthropogenic emission residues on the Himalayan glaciers has been linked to enhanced rates of glacier melting. As a consequence, the ambient air at high altitude Himalayan sites has been monitored intensively over recent decades for its suspended particulates, greenhouse gases, and aerosols emitted from diverse anthropogenic sources (Ran et al., 2014; Rupakheti et al., 2017; Shrestha et al., 2010; Stockwell et al., 2016).

Among the particulate impurities deposited on glacier surface, organic carbon (OC), black carbon (BC), trace metals and biogenic pollutants are the major focus of current research due to their adverse impact on glacier health (Beaudon et al., 2017; Gabrielli et al., 2020; Hong et al., 2009; Kaspari et al., 2011; Nizam et al., 2020; Yan et al., 2019). Himalayan ice core record shows a threefold increase in BC concentrations between 1975 and 2000 (Kaspari et al., 2011). Similarly, increased anthropogenic metal pollution on glaciers has also been reported from several parts of the central Himalaya and Tibetan Plateau (Beaudon et al., 2017; Gabrielli et al., 2020; Hong et al., 2009; Zhang et al., 2009). Despite the rise in BC concentrations and anthropogenic metal pollution, the concentration of inorganic impurities in the western Himalayan glaciers remains poorly known.

Existing data from the western Himalayan region focus mainly on the source of pollutants (CO_x , NO_x , SO_2 , BC, and $\text{PM}_{2.5}$) using emission inventories and receptor and chemical transport modeling (Alvarado et al., 2018; Bonasoni et al., 2010; Rupakheti et al., 2018; Yarragunta et al., 2020). Although these models provide invaluable insights into the abundance, origin, source, and transport pathways of the pollutants over the western Himalayan cryosphere, the results exhibit disagreement between different inventory observations as well as with model results due to the large uncertainties in emission inventory and meteorological parameters. For instance, emission inventory models deployed over South Asia suggest that biofuel burning accounts for 50%–90% of total emissions (Gustafsson et al., 2009 and references therein). Yet, these inventory models are hampered by large uncertainties, in some cases by more than 40% depending upon inventories type, endmember composition, in situ meteorology and inherent model uncertainties. Therefore, given that the Himalaya is neighbored by some of the world's largest emitters of anthropogenic particles, understanding the concentration, origin, and transport pathways of other anthropogenically emitted particles, such as metals, is required to ultimately understand the mechanisms driving enhanced rates of glacier wastage and its impact on downstream populations.

Thus, to establish the contribution of emission sources to the western Himalayan glaciers, we utilize major and trace element geochemistry together with osmium (Os) isotope systematic ($^{187}\text{Os}/^{188}\text{Os}$) of glacier surface impurities. The Os-isotope composition of natural and anthropogenic materials only records the time-integrated fractionation of the Re/Os ratio in the sources. Due to the extremely long half-life of ^{187}Re (ca. 42 billion years), the present-day $^{187}\text{Os}/^{188}\text{Os}$ composition of natural and anthropogenic materials remains practically constant throughout the process of particle generation, transportation, and deposition. As a result, the Re-Os isotopic system is an emerging tool widely used in tracing sources of anthropogenic pollutants in precipitation, snow, and ice in remote regions (Chen et al., 2009; Rauch et al., 2005; Rodushkin et al., 2007; Sen et al., 2013), as well as marine systems (Ownsworth et al., 2019; Sproson et al., 2020). As such, the objective of the study is to apply major and trace element geochemistry, coupled with $^{187}\text{Os}/^{188}\text{Os}$ compositions of cryoconite and moraine samples to constrain the metal composition across the ablation zone of the Chhota Shigri Glacier (CSG) in the western Himalaya. The latter is used to evaluate and discuss the sources of the metal impurities on the ablation zone of CSG and their role in determining rates and mechanisms of glacier mass wasting.

2. Materials and Methods

2.1. Sample Collection

Twenty samples of supraglacial cryoconite were collected from cryoconite holes across the ablation zone of the CSG between 4,500 to 4,930 m a.s.l. (Supporting Information S1 and S2 and Figure S1). The light gray to black colored sediments was collected into Corning® 50 mL centrifuge tube using pre-cleaned plastic scoops. In addition to the cryoconite samples, seven 0.3–0.5 kg samples of moraine debris containing particles ranging in size from clay to cobbles were also collected in polyethylene sterile Whirl-Pack® bags. All samples were kept frozen prior to analysis. To evaluate the presence of anthropogenic emission particulates in the CSG, samples of Gondwana and Tertiary coal from two major Indian coalfields (Jharia in the state of Jharkhand and Makum in the state of Assam), and diesel engine exhaust particulates obtained from engine-exhaust experiments were also analyzed (Supporting Information S3).

2.2. Rhenium-Osmium (Re-Os) Analysis

Cryoconite and moraine samples were dried, sieved (moraine only) and powdered for geochemical analysis (details in Supporting Information S4). 10 samples of cryoconite, two of moraine (<63 μm fraction), four of coal, and two of engine exhaust were selected for Re-Os analysis. The Re-Os concentration and isotopic compositions were determined at the Durham Geochemistry Center using aqua regia carius-tube digestion isotope-dilution negative ion mass spectrometry analytical protocols (Cumming et al., 2013; Selby et al., 2009). Approximately, 1 g of cryoconite and moraine, 0.2 g of coal, and 0.02–0.03 g of exhaust particulate were loaded into a carius tube with a known amount of mixed tracer solution (spike) of ^{190}Os and ^{185}Re and 9 ml of aqua regia solution. The carius tube was sealed and heated to 240°C for 48 h. The Os in the samples digested was isolated and purified using standard solvent extraction (CHCl_3) and micro-distillation

(CrO₃-H₂SO₄-HBr). The Re fraction was isolated and purified using NaOH-acetone solvent extraction and anion chromatography. The isolated Re and Os fractions were loaded onto Ni and Pt filament; with the isotopic composition determined by negative thermal ionization mass spectrometry using a Thermo Fisher TRITON mass spectrometer via static Faraday collection mode for Re and ion-counting using a secondary electron multiplier in the peak-hopping mode for Os. Total procedural blanks were 2.1 ± 0.02 and 0.1 ± 0.01 ppt for Re and Os, respectively, with an average $^{187}\text{Os}/^{188}\text{Os}$ value of 0.25 ± 0.03 ($n = 2$) for cryoconite and moraine analysis, and 2.3 ± 0.2 and 0.1 ± 0.02 ppt for Re and Os, respectively, with an average $^{187}\text{Os}/^{188}\text{Os}$ value of 0.20 ± 0.06 ($n = 4$) for coal and exhaust particulate analysis. In-house standard solution measurements yielded a $^{185}\text{Re}/^{187}\text{Re}$ value of 0.59786 ± 0.00014 (1 SD, $n = 7$) for the Re solution and a $^{187}\text{Os}/^{188}\text{Os}$ value of 0.16085 ± 0.00017 (1 SD, $n = 6$) for the Durham Romil Osmium Solution (DROsS), which agree with those of previous studies (Percival et al., 2019). The average value plus uncertainty of the Re standard solution together with the natural $^{185}\text{Re}/^{187}\text{Re}$ value of 0.5974 (Gramlich et al., 1973) is used for the Re sample mass fractionation correction. Data reduction includes the instrumental mass fractionation, isobaric oxygen interference, and contribution of blanks and the tracer solution. The final two-sigma uncertainties of the Re-Os data include the fully propagated uncertainties of sample-spike weighing, tracer calibration, blank abundances, and isotope compositions, and the intermediate precision of the repeated measurements on the Re and Os reference solutions.

3. Results

3.1. Trace Element Systematics

Trace element concentrations of the cryoconite, bulk moraine (<3 mm, see Supporting Information S4 for details), and fine moraine (<63 μm) fraction normalized to the local rock composition are shown in Figure S2. The fine moraine fractions and cryoconite exhibit similar patterns but possess higher trace element concentrations in comparison to the bulk moraine fractions that resemble local rock compositions. The fine moraine fraction shows higher trace element concentrations than bulk moraine much likely due to additional contamination or mixing of different grain size fractions. This is evident from the negative correlation of SiO₂ with heavy metals including Sc, Ga, Sr, Nb, and Ta (except Pb) (Pearson correlation coefficients $R \geq -0.70$ to -0.94 , $p = 0.001$ – 0.05 ; Figures S3a and S4) (Cai et al., 2015; Thorpe et al., 2019). Additionally, an overall negative correlation is exhibited between other elements (except Li, Be, Rb, Cs, and Ba) against SiO₂. A similar relationship is exhibited between trace metals and SiO₂ in cryoconite samples (Figure S3b). In comparison to the fine moraine fraction, the cryoconite samples exhibit higher concentrations of V, Cr, Co, Ni, and Cd in more than 50% of the samples. Chondrite normalized REE concentrations show LREE enrichment and a negative Eu anomaly for cryoconite and all moraine fractions (Figure S5).

The relationship of the cryoconite trace element ratios to the local rock composition suggests that the cryoconite material has a local crustal provenance. For example, Cd/Zn (0.001–0.007) and Pb/Cu (0.84–1.98) ratios are similar to that of the local rock signature (Cd/Zn = 0.001–0.014 and Pb/Cu = 0.45–5.87). Further, REE ratios including, La/Ce, La/Sm, La/Yb and La/Lu ratios of cryoconite that vary between 0.44–0.51, 30–57, 15–26, and 106–194, respectively, are similar to local rock values (0.37–0.48, 33–91, 15–41, and 113–317, respectively). Noteworthy, the La/Ce, La/Sm, La/Yb, and La/Lu ratios of cryoconite and moraine are much lower than anthropogenic emission sources (La/Ce = 1.3–1.8, La/Sm = 19–28, La/Yb = 135–950, La/Lu = 5400–1000) (Kitto et al., 1992; Olmez & Gordon, 1985) as are the Co/Cs ratios in the cryoconite samples (0.25–2.85, average = 1.12 ± 0.78 , vs. >2.5 for anthropogenic emissions) (Geagea et al., 2007). Further, with the exception to Cr, Ni, and Cd, the enrichment factors (EF) values of ≤ 1 support a predominant crustal provenance for the cryoconite (Figure S6). The EF values for Cr (2.2), Ni (2.7), and Cd (2.6) in cryoconite show a detectable noncrustal input probably attributed to transported anthropogenic particulate metals. However, the Ni, Cr, Cd enrichment is quite low and much likely driven through grain size sorting effect as evident in the fine moraine fraction as well.

3.2. Re-Os Systematics

Rhenium and Os concentrations of the cryoconite, moraine, coal, and vehicular exhaust samples are reported in Table S1. In Figure 1a, the Re (ppb) and Os (ppt) concentrations together with total organic carbon

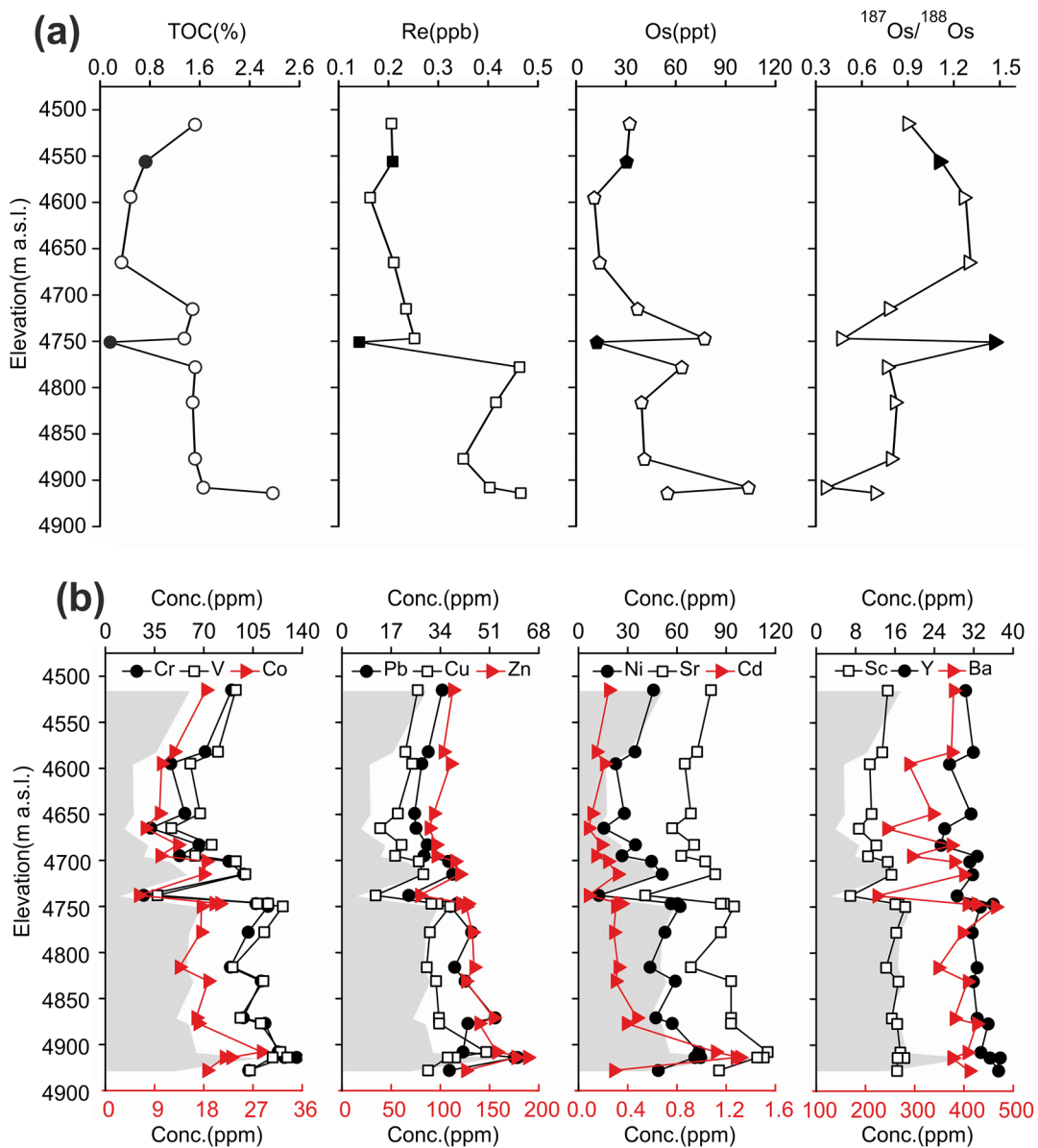


Figure 1. (a) Rhenium-Osmium concentration, $^{187}\text{Os}/^{188}\text{Os}$ ratios and Total Organic Carbon (TOC) in cryoconite (open symbols) and fine moraine fraction (<63 μm , filled symbols) (b) Trace metal concentration in cryoconite and TOC (scale is identical to figure a) along the ablation zone of the CSG. TOC data are from (Nizam et al., 2020).

(TOC; wt %) are shown for cryoconite and the fine moraine fraction. Overall, cryoconite sampled between 4,700–4,930 m a.s.l. has a higher average TOC (~1.7%), Re (0.24–0.47 ppb), and Os (37–104 ppt) content than cryoconite sampled between 4,500 and 4,700 m a.s.l. (average TOC = 0.8%; Re = 0.16–0.21 ppb; Os = 11–32 ppt). The elevated TOC, Re, and Os concentrations in cryoconite sampled from locations above 4,700 m a.s.l. also correspond to higher concentrations of heavy metals (Figure 1b). For example, trace metals such as Cr, V, Co, Cu, and Zn follow the trends shown by Re and Os suggesting that the elemental enrichment is probably controlled by common (chelating) mechanism/sources (Chen et al., 2016). The absolute abundances of Re and Os show a moderate positive correlation with each other ($R = 0.58$, $p = 0.1$) (Figures S3b and S7), and similar correlation with TOC ($R = 0.71$ and 0.53 respectively). The cryoconite $^{187}\text{Os}/^{188}\text{Os}$ composition falls between 0.38 and 1.31, with cryoconite from sites between 4,700 and 4,930 m a.s.l. possessing $^{187}\text{Os}/^{188}\text{Os}$ values between 0.38 and 0.83. Cryoconite samples from below 4,700 m a.s.l. have more radiogenic $^{187}\text{Os}/^{188}\text{Os}$ values. The $^{187}\text{Os}/^{188}\text{Os}$ ratios show a significant negative correlation with Os concentrations

($R = -0.94$, $p = 0.001$; Figures S3b and S7). Further, the $^{187}\text{Os}/^{188}\text{Os}$ ratios correlate positively with major oxides such as SiO_2 , Na_2O , and K_2O ($R = 0.71$ – 0.89 , $p = 0.001$ – 0.05). In contrast, heavy REE (HREE: Er to Lu), MgO , Fe_2O_3 , MnO , and TiO_2 exhibit a significant negative correlation with $^{187}\text{Os}/^{188}\text{Os}$ ratios ($R = -0.81$ to -0.93 , $p = 0.001$ – 0.01 ; Figures S7 and S8).

The Re and Os concentrations of two moraine samples from $\sim 4,750$ and $4,550$ m a.s.l are 0.14 and 0.21 ppb and 13 and 30 ppt, being similar to the average upper continental crust (UCC) composition (Re = ~ 0.20 ppb; Os = ~ 31 ppt) (Esser & Turekian, 1993; Peucker-Ehrenbrink & Jahn, 2001). The Re and Os concentrations in Gondwana coal range between 0.26 and 0.76 ppb and 7 and 18 ppt, respectively. The Re and Os concentrations in Tertiary coal samples range between 0.47 and 0.53 ppb and 63 and 726 ppt respectively. Unlike cryoconite, the Gondwana and Tertiary coals show limited variability and are characterized by radiogenic ($^{187}\text{Os}/^{188}\text{Os} = 1.61$ – 1.64) and unradiogenic osmium isotope compositions ($^{187}\text{Os}/^{188}\text{Os} = 0.14$ and 0.21), respectively. The analysis of two engine exhausts yielded Re and Os concentrations of 0.07 and 1.04 ppb and 2 and 6 ppt, respectively. The engine exhaust samples are characterized by an unradiogenic osmium isotope composition ($^{187}\text{Os}/^{188}\text{Os} = 0.21$ – 0.22), similar to catalytic converters (Poirier & Gariépy, 2005).

4. Discussion

4.1. Cryoconite Provenance

Glaciers are sites of active physical erosion, with their continuous movement effectively powdering rock units in the glacial catchment that can be further eroded by wind action and deflation (Brown et al., 1996; Sharp et al., 1995; Tranter et al., 2002). This local freshly weathered rock that is subjected to deflation will overwhelm any long-range dust transport signal by covering the neighbouring glacier. This is illustrated by both the major (Figure S9) and trace element systematics (Figure S2) of the CSG cryoconite, which are derived from weakly weathered rocks of the glacial catchment. Most of the cryoconite (14 samples) exhibit Co, Cr, Ni, and Sc enrichment that indicates a detectable noncrustal component. In contrast, cryoconite from Arctic, European, Canadian, and other South Asian glaciers exhibits heavy metal enrichment several orders of magnitude higher than were found in their local rock and moraine, which is consistent with high activity concentrations of anthropogenic radionuclides (Baccolo et al., 2017; Beaudon et al., 2017; Łokas et al., 2016; Owens et al., 2019; Singh et al., 2013). This suggests that the CSG can be classified as being relatively pristine compared to other glaciers on which significant anthropogenic pollution signal has been recorded and linked to long-range transport of the anthropogenic emission residues. Moreover, samples showing detectable metals enrichment occurs mainly in the upper reaches (except first sample) of the CSG ablation zone, that is, above $4,700$ m a.s.l. Additionally, these samples show minor deviation from the local moraine composition toward a more mafic rock composition (Figures S10 and S11). Although heavy metal enrichment can also be attributed to anthropogenic contributions, the correlation with TOC suggests that enrichment is most plausibly attributed to sources of TOC (microorganisms) owing to their inherent tendency to accumulate fine chelate metals (Łokas et al., 2016). Furthermore, given that air-mass back trajectory modeling clearly shows that 50% of the air mass that reaches the CSG originates from the west, within ~ 250 km of the study site and possesses limited inputs from the Indo-Gangetic Basin (Nizam et al., 2020), only minor input from anthropogenic sources can be considered. Lastly, the chondrite normalized REE signature of moraine, local country rocks from the Himalaya, river sediments from glacial catchments, cryoconite, snow, and ice core dust (Figure S12) show similar REE patterns, all exhibiting REE enrichment similar to that of granitic or shale (PAAS)-like sources, which are commonly observed in the Higher and the Lesser Himalayan rocks and sediment. The anthropogenic dust mostly exhibits fractionated (enriched) LREE patterns with smooth HREE enrichment and often contains a strong positive Gd anomaly (Geagea et al., 2007; Hatje et al., 2016). The cryoconite shows a large range of $^{187}\text{Os}/^{188}\text{Os}$ compositions (0.4 – 1.3) that overlaps with both natural and anthropogenic sources (Figure 2).

The unradiogenic $^{187}\text{Os}/^{188}\text{Os}$ signature of cryoconite (~ 0.4) could be explained by contributions from both natural Os sources such as cosmic dust, volcanic aerosols, mafic and ultramafic rocks, and anthropogenic Os from catalytic converters that are often recycled ($^{187}\text{Os}/^{188}\text{Os} = \sim 0.38$) (Poirier & Gariépy, 2005) and from fossil fuels, smelting of chromite, base-metal sulfide, PGE ores, and municipal solid waste incinerators (MSWIs). Contributions from volcanic aerosols and cosmic dust seem unlikely due to the absence of active volcanism in and around the Himalaya and extremely low ($40,000 \pm 20,000$ t yr $^{-1}$; $t = 10^6$ g) global

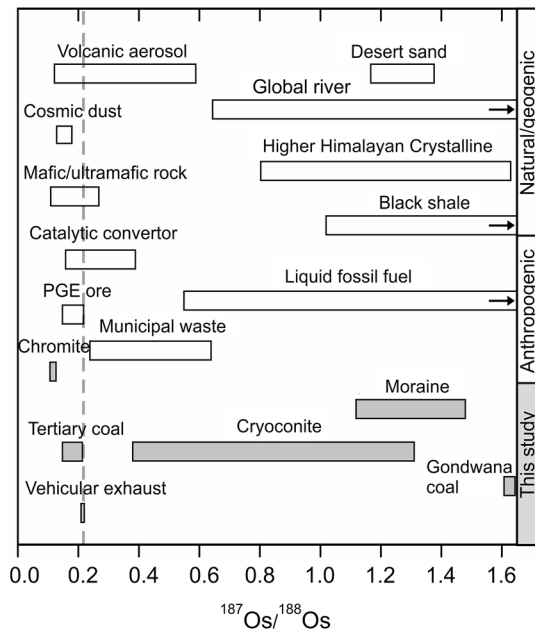


Figure 2. Comparison of osmium isotopic ratio of cryoconite and moraine with different potential sources. The dashed vertical line marks the limit of the measured unradiogenic Os that can be directly contributed by vehicular emission in the atmosphere. Moraine Os isotopic ratios lie within the crustal range of both eroding, that is, global river (Levasseur et al., 1999) and noneroding crust: Higher Himalayan Crystalline Sequence (Pierson-Wickmann et al., 2000), black shale (Ackerman et al., 2019; Selby & Creaser, 2003; Singh et al., 1999; van Acken et al., 2019). Cryoconite, in contrast, exhibits a range in $^{187}\text{Os}/^{188}\text{Os}$ ratios that encompass crustal to unradiogenic signature similar to that of recycled catalytic converters (Poirier & Gariépy, 2005), volcanic aerosol (Krähenbühl et al., 1992; Yudovskaya et al., 2008), and municipal waste (Funari et al., 2016). Data reference: cosmic dust (Schmitz et al., 1997; Walker et al., 2002), mafic/ultramafic rock (Hanski et al., 2001; Meisel et al., 2001), Taklimakan desert and Kunlun moraine (Hattori et al., 2003), catalytic convertor (Poirier & Gariépy, 2005), liquid fossil fuel (Corrick et al., 2019; Cumming et al., 2014; Lillis & Selby, 2013; Selby et al., 2007), chromite ore (Mondal et al., 2007), PGE ore (Coggon et al., 2012), and municipal waste (Funari et al., 2016).

cosmic dust flux (Love & Brownlee, 1993) that can significantly affect the $^{187}\text{Os}/^{188}\text{Os}$ of sediments in the highly active glacial ablation zones. However, a contribution from mafic rocks is plausible as ultramafic dykes, sills, and pegmatitic veins (early Proterozoic-late Paleozoic age) are common in Higher Himalayan Crystalline Sequence (HHCS) and locally in the glacial catchment (Thakur & Patel, 2012; Thöni et al., 2012). Given that the unradiogenic $^{187}\text{Os}/^{188}\text{Os}$ signature in the cryoconite correlates with high Fe_2O_3 -MgO and low SiO_2 concentrations (Figure S8), a mafic/ultramafic source rock input is likely instead of anthropogenic input and is supported by the cryoconite trace element geochemistry. Therefore, from trace element systematics, Re and Os concentrations, and $^{187}\text{Os}/^{188}\text{Os}$ compositions it can be concluded that the glacial debris contains felsic and mafic/ultramafic rock components, with essentially no input from anthropogenic sources.

4.2. Further Evaluation of Natural and Anthropogenic Sourced Osmium

The relative contributions from various source endmembers are quantified using a three-component mixing model using $^{187}\text{Os}/^{188}\text{Os}$ and Os concentration as tracers. The first end-member represents local rocks, which are very similar in composition to the HHCS (Pierson-Wickmann et al., 2000) and eroding UCC (Peucker-Ehrenbrink & Jahn, 2001) for which we assign an Os abundance of 30.4 ppt and $^{187}\text{Os}/^{188}\text{Os}$ value of ~ 1.48 (Table S1). For the second end-member, mafic-ultramafic rocks are selected having an Os concentration of 850 ppt and an $^{187}\text{Os}/^{188}\text{Os}$ value of ~ 0.12 (Table 4; Data from Meisel et al., 2001, sample number: KH80-100, peridotite xenoliths). To explain the data distribution (Figure 3a), the third endmember should have low Os concentration and an intermediate $^{187}\text{Os}/^{188}\text{Os}$ composition. This end-member could represent an Os-poor mineral such as aeolian quartz or granitoid and/or gneisses (Peucker-Ehrenbrink & Blum, 1998). We therefore assign an Os concentration of 1 ppt and a $^{187}\text{Os}/^{188}\text{Os}$ value of ~ 0.90 . It is noteworthy that the $^{187}\text{Os}/^{188}\text{Os}$ composition could be more radiogenic and Os concentrations could be significantly lesser (Peucker-Ehrenbrink & Blum, 1998). Keeping in mind that the three end-members of our mixing model with the defined endmembers should enclose all data points (Figure 3a), we performed our mixing model with the defined endmembers as outlined above. Our mixing calculations suggest that the cryoconite $^{187}\text{Os}/^{188}\text{Os}$ signature is mainly derived from local rocks ($67.4 \pm 18.6\%$), and Os-poor mineral phase ($29.6 \pm 19.9\%$), with limited input from the mafic-ultramafic rocks ($3.0 \pm 2.8\%$, Figure 3b). In general, the upper elevation of the glacier showed a greater Os contribution from mafic rock/mineral phases, which is consistent with the trace element systematics (Figure 1b).

We acknowledge that the choice of end-member compositions will change the end-member contributions, but we emphasize that the conclusion of the study will not change. Further, we did not include any anthropogenic sources because enrichment factors and trace and major element concentrations support a predominantly crustal provenance for the cryoconite. Moreover, this is supported by the fact that the glacier ablation zone is mostly free of fossil fuel derived carbon (Nizam et al., 2020). We did not, therefore, include coal and engine exhaust as suitable endmembers. We also emphasize that the metal enrichment in the cryoconite can be influenced by microbial processes. Given the elevated TOC concentration observed in upper ablation zone of the CSG, a higher level of microbial activity is implied (Anesio et al., 2009). The $\delta^{13}\text{C}$ enrichment (-18.19%) in cryoconite samples and its relationship with N enrichment and or depletion supports contributions from photo-autotrophic and heterotrophic micro-organisms that may also have modified predominantly heavy metal (Cr, V, Ni, and Co) signature (Nizam et al., 2020).

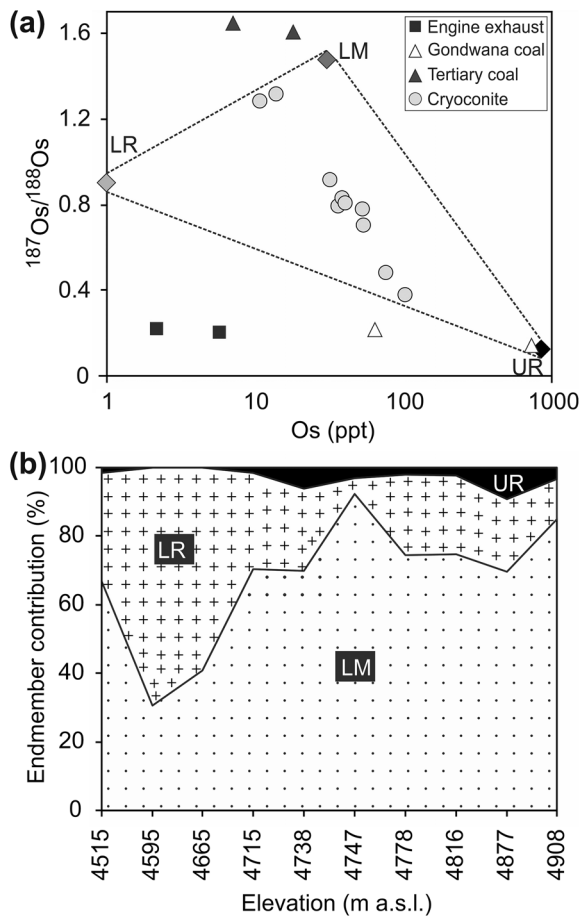


Figure 3. (a) Three-component mixing modeling plot for Os concentration and $^{187}\text{Os}/^{188}\text{Os}$ for cryoconite and the proposed three end-members: LM (Local Moraine), LR (Less Radiogenic Os poor mineral phase: aeolian quartz/granite/orthogneiss), and UR (Ultramafic Rocks). (b) Percent contribution of the Os sources in cryoconite with elevation along the ablation zone of the Chhota Shigri Glacier. See text for discussion.

4.3. Implications of the Absence of Anthropogenic Emission Residues From the Western Himalayan Glacier

Glaciers receive a large supply of metals in the form of windblown mineral dust from the erosion of the UCC and mafic rocks, with inputs from anthropogenic sources (Casey, 2012; Cristofanelli et al., 2014; Wake et al., 1993). Knowledge of the amount, composition, and source of dust and anthropogenic emissions is essential to calculate the heat-absorbing capacity of the residue, and in turn, ice melting rates. For example, 1 ppb of BC residue on the glacier has the same effect on albedo as that of 75 ppb dust (Jacobi et al., 2015). In this study, we show that CSG debris contains negligible impurity contributions from fossil fuel emission sources. Further, carbon characterization (Ramped Pyrolysis Oxidation: RPO, $\delta^{13}\text{C}$, and ^{14}C chronology) of TOC in both cryoconite and the $<63\ \mu\text{m}$ (fine) fraction of moraine from the same glacier revealed that the cryoconite has negligible contributions from fossil fuel emission sources (Nizam et al., 2020). The RPO, $\delta^{13}\text{C}$, and ^{14}C data reveal that $98.3 \pm 1.6\%$ of the OC is sourced from local biomass sources, atmospheric organic matter, and glacial microbes, with only $1.7 \pm 1.6\%$ of the OC being sourced from petrogenetic sources. Further, it has been shown that, on annual basis, 50% of the air mass originates from far ($>1,000\ \text{km}$) to the west of the receptor site (CSG) Nizam et al. (2020). Therefore, based on the Os isotopic systematics and previous findings we conclude that the CSG is essentially free of anthropogenic residues and receives limited long-range dust inputs.

It is well established that glaciers in the CSG basin have been losing mass at an average rate of 0.50 meter water-equivalent per year (m w.e. yr^{-1}) over the last two decades (Azam et al., 2019), which is relatively higher than the regional rate of loss from glaciers in the central (0.35 m w.e. yr^{-1}) and eastern Himalaya (0.43 m w.e. yr^{-1}), having more extensive debris cover (18%–24%) and substantial inputs of anthropogenically sourced pollutants from the Indian subcontinent (Babu et al., 2011; Brun et al., 2017; Li et al., 2016). The high glacial mass wastage rate observed in the western Himalaya is likely due to a mean annual tropospheric warming trend ($0.016 \pm 0.005\ \text{K}\ \text{yr}^{-1}$) during ablation season, which is higher than that found in the central and eastern Himalayan region (Prasad et al., 2009). Consequently, warming-induced melting of snow (which is

80% of total precipitation) constitutes the large fraction (15%–66%) of the annual hydrological budget in the western Himalaya (Azam et al., 2019; Bookhagen & Burbank, 2010). In contrast, central and western Himalayan glaciers are fed by the Indian Summer Monsoon (which contributes $\sim 80\%$ of the annual hydrological budget) and receive a significant fraction of anthropogenic pollutants (50% of total anthropogenic carbon) from the heavily polluted Indo-Gangetic Plain (Li et al., 2016) that can enhance melting by $340\ \text{kg}\ \text{m}^{-2}\ \text{yr}^{-1}$ (Ginot et al., 2014). However, other surface darkening factors such as presence of pigmented microbes, detrital organic matter, accumulations of particulates on the glacier surface may also enhance the glacial melting and cannot be ruled out without further research.

Therefore the near absence of anthropogenic particles on the nearly debris free CSG reveals that any heat-absorbing anthropogenic particles deposited on the surface of the CSG are not one of the primary drivers behind CSG melting, as observed on glaciers in other parts of the world, such as Greenland, Alaska, and Tibet (Dumont et al., 2014; Nagorski et al., 2019; Xu et al., 2009). Despite an increase in anthropogenic emissions from the Indian subcontinent over the last 50 years (Crippa et al., 2018), we conclude that anthropogenic emission residues (due to negligible occurrence) on the surface of CSG might not significantly enhance glacier mass wastage rates in the near future. The rapid retreat of CSG can be best explained by rising air temperatures, and morphological characteristics of the CSG catchment. It is noteworthy that numerical modeling (under RCP 8.6 climatic scenario, see Chaturvedi, et al., 2014 for details) of the surface

mass balance of CSG reveals that the glacier will cease to exist by 2109 CE with a temperature rise of 5.5 K from the local mean annual temperature of the year 2009 (Gantayat et al., 2017).

5. Conclusion

The concentration, origin, and depositional pathways of metals on the CSG were investigated for the first time using major and trace elements, and Re-Os isotope systematic of debris samples from supraglacial cryoconite holes and moraines. Our study highlights two important points regarding the presence of metal impurities on the CSG surface. First, although the Himalaya is surrounded by some of the world's largest emitters of anthropogenic particles, however, we find limited evidence for anthropogenic metal impurities on the CSG likely due to the source region of the air mass reaching the CSG mainly coming from west. Mixing model calculations show that Os in the CSG is exclusively sourced from local crustal rocks. Second, integration of geochemical and air-mass back trajectory modeling data reveals that the sediment/dust is mostly of local origin. We conclude that the impact of anthropogenic particulate emission on the CSG melting is limited and caused by climate warming and other glacier surface darkening factors viz., presence of pigmented microbial cells, detrital organic matter, OC from local biomass sources, and natural dust/debris cover. Therefore, future glacial melt modeling studies should include the anthropogenic emission impurities for clean glaciers like CSG with caution.

Conflict of Interest

The authors declare no conflicts of interest relevant to this study.

Data Availability Statement

All of the original data set used in the study are publicly available at <https://doi.org/10.6084/m9.figshare.15177441.v1>.

Acknowledgments

This project is financially supported by Department of Science and Technology, Government of India, Climate Change Program (SPLICE) Grant DST/CCP/Aerosol/86/2017(C) and Science & Engineering Research Board (SERB) Grant (EMR/2015/000439) to I.S. Sen. S. Nizam is thankful to Indian Institute of Technology-Kanpur (IIT-Kanpur) for Ph.D. scholarship. The authors thank IIT-Kanpur and Durham University for providing access to instrumentation and support. They are thankful to Mohd Farooq Azam from IIT Indore for field sampling support. Sincere thanks to A. K. Agarwal to provide access to the Engine Research Lab. Discussion with Michael Bizimis, Thomas Meisel, Arijeet Mitra and Soumita Boral greatly acknowledged. D. Selby acknowledges the technical support of Chris Ottley, Geoff Nowell, and Antonia Hofmann, and also the support of the TOTAL Endowment Fund and the Dida Scholarship of CUG.

References

- Ackerman, L., Pašava, J., Šípková, A., Martínková, E., Haluzová, E., Rodovská, Z., & Chrástný, V. (2019). Copper, zinc, chromium and osmium isotopic compositions of the Teplá-Barrandian unit black shales and implications for the composition and oxygenation of the Neoproterozoic-Cambrian ocean. *Chemical Geology*, 521, 59–75. <https://doi.org/10.1016/j.chemgeo.2019.05.013>
- Alvarado, M. J., Winijkul, E., Adams-Selin, R., Hunt, E., Brodowski, C., Lonsdale, C. R., et al. (2018). Sources of Black Carbon Deposition to the Himalayan Glaciers in Current and Future Climates. *Journal of Geophysical Research: Atmospheres*, 123(14), 7482–7505. <https://doi.org/10.1029/2018JD029049>
- Anesio, A. M., Hodson, A. J., Fritz, A., Psenner, R., & Sattler, B. (2009). High microbial activity on glaciers: Importance to the global carbon cycle. *Global Change Biology*, 15(4), 955–960. <https://doi.org/10.1111/j.1365-2486.2008.01758.x>
- Azam, M. F., Wagnon, P., Vincent, C., Ramanathan, A., Favier, V., Mandal, A., & Pottakkal, J. G. (2014). Processes governing the mass balance of Chhota Shigri Glacier (western Himalaya, India) assessed by point-scale surface energy balance measurements. *The Cryosphere*, 8(6), 2195–2217. <https://doi.org/10.5194/tc-8-2195-2014>
- Azam, M. F., Wagnon, P., Vincent, C., Ramanathan, A., Kumar, N., Srivastava, S., et al. (2019). Snow and ice melt contributions in a highly glacierized catchment of Chhota Shigri Glacier (India) over the last five decades. *Journal of Hydrology*, 574, 760–773. <https://doi.org/10.1016/j.jhydrol.2019.04.075>
- Babu, S. S., Chaubey, J. P., Krishna Moorthy, K., Gogoi, M. M., Kompalli, S. K., Sreekanth, V., et al. (2011). High altitude (~4520 m amsl) measurements of black carbon aerosols over western trans-Himalayas: Seasonal heterogeneity and source apportionment. *Journal of Geophysical Research*, 116(D24), 0. <https://doi.org/10.1029/2011JD016722>
- Baccolo, G., Di Mauro, B., Massabò, D., Clemenza, M., Nastasi, M., Delmonte, B., et al. (2017). Cryoconite as a temporary sink for anthropogenic species stored in glaciers. *Scientific Reports*, 7(1), 9623. <https://doi.org/10.1038/s41598-017-10220-5>
- Beaudon, E., Gabrielli, P., Sierra-Hernández, M. R., Wegner, A., & Thompson, L. G. (2017). Central Tibetan Plateau atmospheric trace metals contamination: A 500-year record from the Puruogangri ice core. *The Science of the Total Environment*, 601–602, 1349–1363. <https://doi.org/10.1016/j.scitotenv.2017.05.195>
- Bonasoni, P., Laj, P., Marinoni, A., Sprenger, M., Angelini, F., Arduini, J., et al. (2010). Atmospheric Brown Clouds in the Himalayas: First two years of continuous observations at the Nepal Climate Observatory-Pyramid (5079 m). *Atmospheric Chemistry and Physics*, 10(15), 7515–7531. <https://doi.org/10.5194/acp-10-7515-2010>
- Bookhagen, B., & Burbank, D. W. (2010). Toward a complete Himalayan hydrological budget: Spatiotemporal distribution of snowmelt and rainfall and their impact on river discharge. *Journal of Geophysical Research*, 115(F3), F03019. <https://doi.org/10.1029/2009JF001426>
- Brown, G. H., Sharp, M., & Tranter, M. (1996). Subglacial chemical erosion: Seasonal variations in solute provenance, Haut Glacier D'Arolla, Valais, Switzerland. *Annals of Glaciology*, 22, 25–31. <https://doi.org/10.3189/1996AoS22-1-25-31>
- Brun, F., Berthier, E., Wagnon, P., Kääh, A., & Treichler, D. (2017). A spatially resolved estimate of High Mountain Asia glacier mass balances from 2000 to 2016. *Nature Geoscience*, 10(9), 668–673. <https://doi.org/10.1038/ngeo2999>

- Cai, L., Xu, Z., Bao, P., He, M., Dou, L., Chen, L., et al. (2015). Multivariate and geostatistical analyses of the spatial distribution and source of arsenic and heavy metals in the agricultural soils in Shunde, Southeast China. *Journal of Geochemical Exploration*, 148, 189–195. <https://doi.org/10.1016/j.gexplo.2014.09.010>
- Casey, K. A. (2012). Supraglacial dust and debris: Geochemical compositions from glaciers in Svalbard, southern Norway, Nepal and New Zealand. *Earth System Science Data Discussions*, 5(1), 107–145. <https://doi.org/10.5194/essdd-5-107-2012>
- Chaturvedi, R. K., Kulkarni, A., Karyakarte, Y., Joshi, J., & Bala, G. (2014). Glacial mass balance changes in the Karakoram and Himalaya based on CMIP5 multi-model climate projections. *Climatic Change*, 123(2), 315–328. <https://doi.org/10.1007/s10584-013-1052-5>
- Chen, C., Sedwick, P. N., & Sharma, M. (2009). Anthropogenic osmium in rain and snow reveals global-scale atmospheric contamination. *Proceedings of the National Academy of Sciences*, 106(19), 7724–7728. <https://doi.org/10.1073/pnas.0811803106>
- Chen, K., Walker, R. J., Rudnick, R. L., Gao, S., Gaschnig, R. M., Puchtel, I. S., et al. (2016). Platinum-group element abundances and Re–Os isotopic systematics of the upper continental crust through time: Evidence from glacial diamictites. *Geochimica et Cosmochimica Acta*, 191, 1–16. <https://doi.org/10.1016/j.gca.2016.07.004>
- Coggon, J. A., Nowell, G. M., Pearson, D. G., Oberthür, T., Lorand, J.-P., Melcher, F., & Parman, S. W. (2012). The 190Pt–186Os decay system applied to dating platinum-group element mineralization of the Bushveld Complex, South Africa. *Chemical Geology*, 302–303, 48–60. <https://doi.org/10.1016/j.chemgeo.2011.10.015>
- Corrick, A. J., Selby, D., McKirdy, D. M., Hall, P. A., Gong, S., Trefry, C., & Ross, A. S. (2019). Remotely constraining the temporal evolution of offshore oil systems. *Scientific Reports*, 9(1), 1327. <https://doi.org/10.1038/s41598-018-37884-x>
- Crippa, M., Guizzardi, D., Muntean, M., Schaaf, E., Dentener, F., van Aardenne, J. A., et al. (2018). Gridded emissions of air pollutants for the period 1970–2012 within EDGAR v4.3.2. *Earth System Science Data*, 10(4), 1987–2013. <https://doi.org/10.5194/essd-10-1987-2018>
- Cristofanelli, P., Putero, D., Adhikary, B., Landi, T. C., Marinoni, A., Duchi, R., et al. (2014). Transport of short-lived climate forcers/pollutants (SLCF/P) to the Himalayas during the South Asian summer monsoon onset. *Environmental Research Letters*, 9(8), 084005. <https://doi.org/10.1088/1748-9326/9/8/084005>
- Cumming, V. M., Poulton, S. W., Rooney, A. D., & Selby, D. (2013). Anoxia in the terrestrial environment during the late Mesoproterozoic. *Geology*, 41(5), 583–586. <https://doi.org/10.1130/G34299.1>
- Cumming, V. M., Selby, D., Lillis, P. G., & Lewan, M. D. (2014). Re–Os geochronology and Os isotope fingerprinting of petroleum sourced from a Type I lacustrine kerogen: Insights from the natural Green River petroleum system in the Uinta Basin and hydrous pyrolysis experiments. *Geochimica et Cosmochimica Acta*, 138, 32–56. <https://doi.org/10.1016/j.gca.2014.04.016>
- Dumont, M., Brun, E., Picard, G., Michou, M., Libois, Q., Petit, J.-R., et al. (2014). Contribution of light-absorbing impurities in snow to Greenland's darkening since 2009. *Nature Geoscience*, 7(7), 509–512. <https://doi.org/10.1038/ngeo2180>
- Esser, B. K., & Turekian, K. K. (1993). The osmium isotopic composition of the continental crust. *Geochimica et Cosmochimica Acta*, 57(13), 3093–3104. [https://doi.org/10.1016/0016-7037\(93\)90296-9](https://doi.org/10.1016/0016-7037(93)90296-9)
- Funari, V., Meisel, T., & Braga, R. (2016). The potential impact of municipal solid waste incinerators ashes on the anthropogenic osmium budget. *The Science of the Total Environment*, 541, 1549–1555. <https://doi.org/10.1016/j.scitotenv.2015.10.014>
- Gabrielli, P., Wegner, A., Sierra-Hernández, M. R., Beaudon, E., Davis, M., Barker, J. D., & Thompson, L. G. (2020). Early atmospheric contamination on the top of the Himalayas since the onset of the European Industrial Revolution. *Proceedings of the National Academy of Sciences*, 117(8), 3967–3973. <https://doi.org/10.1073/pnas.1910485117>
- Gantayat, P., Kulkarni, A. V., Srinivasan, J., & Schmeits, M. J. (2017). Numerical modelling of past retreat and future evolution of Chhota Shigri glacier in Western Indian Himalaya. *Annals of Glaciology*, 58(75pt2), 136–144. <https://doi.org/10.1017/aog.2017.21>
- Geagea, M. L., Stille, P., Millet, M., & Perrone, T. (2007). REE characteristics and Pb, Sr and Nd isotopic compositions of steel plant emissions. *The Science of the Total Environment*, 373(1), 404–419. <https://doi.org/10.1016/j.scitotenv.2006.11.011>
- Ginot, P., Dumont, M., Lim, S., Patris, N., Taupin, J. D., Wagnon, P., et al. (2014). A 10 year record of black carbon and dust from a Mera Peak ice core (Nepal): Variability and potential impact on melting of Himalayan glaciers. *The Cryosphere*, 8(4), 1479–1496. <https://doi.org/10.5194/tc-8-1479-2014>
- Gramlich, J. W., Murphy, T. J., Garner, E. L., & Shields, W. R. (1973). Absolute isotopic abundance ratio and atomic weight of a reference sample of rhenium. *Journal of Research of the National Bureau of Standards Section A: Physics and Chemistry*, 77A(6), 691. <https://doi.org/10.6028/jres.077A.040>
- Gustafsson, O., Krusa, M., Zencak, Z., Sheesley, R. J., Granat, L., Engstrom, E., et al. (2009). Brown Clouds over South Asia: Biomass or Fossil Fuel Combustion? *Science*, 323(5913), 495–498. <https://doi.org/10.1126/science.1164857>
- Hanski, E., Walker, R. J., Huhma, H., & Suominen, I. (2001). The Os and Nd isotopic systematics of c. 2.44 Ga Akanvaara and Koitelainen mafic layered intrusions in northern Finland. *Precambrian Research*, 109(1–2), 73–102. [https://doi.org/10.1016/S0301-9268\(01\)00142-5](https://doi.org/10.1016/S0301-9268(01)00142-5)
- Hatje, V., Bruland, K. W., & Flegal, A. R. (2016). Increases in anthropogenic gadolinium anomalies and rare earth element concentrations in San Francisco Bay over a 20 year record. *Environmental Science & Technology*, 50(8), 4159–4168. <https://doi.org/10.1021/acs.est.5b04322>
- Hattori, Y., Suzuki, K., Honda, M., & Shimizu, H. (2003). Re–os isotope systematics of the Taklimakan Desert sands, moraines and river sediments around the Taklimakan Desert, and of Tibetan soils. *Geochimica et Cosmochimica Acta*, 67(6), 1195–1205. [https://doi.org/10.1016/S0016-7037\(00\)01206-1](https://doi.org/10.1016/S0016-7037(00)01206-1)
- Hong, S., Lee, K., Hou, S., Hur, S. D., Ren, J., Burn, L. J., et al. (2009). An 800-YEAR RECORD OF ATMOSPHERIC As, Mo, Sn, and Sb in Central Asia in high-altitude ice cores from Mt. Qomolangma (Everest), Himalayas. *Environmental Science & Technology*, 43(21), 8060–8065. <https://doi.org/10.1021/es901685u>
- Jacobi, H.-W., Lim, S., Ménéguez, M., Ginot, P., Laj, P., Bonasoni, P., et al. (2015). Black carbon in snow in the upper Himalayan Khumbu Valley, Nepal: Observations and modeling of the impact on snow albedo, melting, and radiative forcing. *The Cryosphere*, 9(4), 1685–1699. <https://doi.org/10.5194/tc-9-1685-2015>
- Kaspari, S. D., Schwikowski, M., Gysel, M., Flanner, M. G., Kang, S., Hou, S., & Mayewski, P. A. (2011). Recent increase in black carbon concentrations from a Mt. Everest ice core spanning 1860–2000 AD. *Geophysical Research Letters*, 38(4), n/a–n/a. <https://doi.org/10.1029/2010GL046096>
- Kitto, M. E., Anderson, D. L., Gordon, G. E., & Olmez, I. (1992). Rare earth distributions in catalysts and airborne particles. *Environmental Science & Technology*, 26(7), 1368–1375. <https://doi.org/10.1021/es00031a014>
- Krähenbühl, U., Geissbühler, M., Bühler, F., Eberhardt, P., & Finnegan, D. L. (1992). Osmium isotopes in the aerosols of the mantle volcano Mauna Loa. *Earth and Planetary Science Letters*, 110(1–4), 95–98. [https://doi.org/10.1016/0012-821X\(92\)90041-S](https://doi.org/10.1016/0012-821X(92)90041-S)
- Levasseur, S., Birck, J.-L., & Allègre, C. J. (1999). The osmium riverine flux and the oceanic mass balance of osmium. *Earth and Planetary Science Letters*, 174(1–2), 7–23. [https://doi.org/10.1016/S0012-821X\(99\)00259-9](https://doi.org/10.1016/S0012-821X(99)00259-9)

- Li, C., Bosch, C., Kang, S., Andersson, A., Chen, P., Zhang, Q., et al. (2016). Sources of black carbon to the Himalayan–Tibetan Plateau glaciers. *Nature Communications*, 7(1), 12574. <https://doi.org/10.1038/ncomms12574>
- Lillis, P. G., & Selby, D. (2013). Evaluation of the rhenium–osmium geochronometer in the Phosphoria petroleum system, Bighorn Basin of Wyoming and Montana, USA. *Geochimica et Cosmochimica Acta*, 118, 312–330. <https://doi.org/10.1016/j.gca.2013.04.021>
- Lokas, E., Zaborska, A., Kolicka, M., Różycki, M., & Zawierucha, K. (2016). Accumulation of atmospheric radionuclides and heavy metals in cryoconite holes on an Arctic glacier. *Chemosphere*, 160, 162–172. <https://doi.org/10.1016/j.chemosphere.2016.06.051>
- Love, S. G., & Brownlee, D. E. (1993). A Direct Measurement of the Terrestrial Mass Accretion Rate of Cosmic Dust. *Science*, 262(5133), 550–553. <https://doi.org/10.1126/science.262.5133.550>
- Meisel, T., Walker, R. J., Irving, A. J., & Lorand, J.-P. (2001). Osmium isotopic compositions of mantle xenoliths: A global perspective. *Geochimica et Cosmochimica Acta*, 65(8), 1311–1323. [https://doi.org/10.1016/S0016-7037\(00\)00566-4](https://doi.org/10.1016/S0016-7037(00)00566-4)
- Mondal, S. K., Frei, R., & Ripley, E. M. (2007). Os isotope systematics of mesoarchean chromitite-PGE deposits in the Singhbhum Craton (India): Implications for the evolution of lithospheric mantle. *Chemical Geology*, 244(3–4), 391–408. <https://doi.org/10.1016/j.chemgeo.2007.06.025>
- Nagorski, S. A., Kaspari, S. D., Hood, E., Fellman, J. B., & Skiles, S. M. (2019). Radiative Forcing by Dust and Black Carbon on the Juneau Icefield, Alaska. *Journal of Geophysical Research: Atmospheres*, 124(7), 3943–3959. <https://doi.org/10.1029/2018JD029411>
- Nizam, S., Sen, I. S., Vinoj, V., Galy, V., Selby, D., Azam, M. F., et al. (2020). Biomass-derived provenance dominates glacial surface organic carbon in the western Himalaya. *Environmental Science & Technology*, 54(14), 8612–8621. <https://doi.org/10.1021/acs.est.0c02710>
- Olmez, I., & Gordon, G. E. (1985). Rare Earths: Atmospheric Signatures for Oil-Fired Power Plants and Refineries. *Science*, 229(4717), 966–968. <https://doi.org/10.1126/science.229.4717.966>
- Owens, P. N., Blake, W. H., & Millward, G. E. (2019). Extreme levels of fallout radionuclides and other contaminants in glacial sediment (cryoconite) and implications for downstream aquatic ecosystems. *Scientific Reports*, 9(1), 12531. <https://doi.org/10.1038/s41598-019-48873-z>
- Owensworth, E., Selby, D., Ottley, C. J., Unsworth, E., Raab, A., Feldmann, J., et al. (2019). Tracing the natural and anthropogenic influence on the trace elemental chemistry of estuarine macroalgae and the implications for human consumption. *The Science of the Total Environment*, 685, 259–272. <https://doi.org/10.1016/j.scitotenv.2019.05.263>
- Percival, L. M. E., Selby, D., Bond, D. P. G., Rakociński, M., Racki, G., Marynowski, L., et al. (2019). Pulses of enhanced continental weathering associated with multiple Late Devonian climate perturbations: Evidence from osmium isotope compositions. *Palaeogeography, Palaeoclimatology, Palaeoecology*, 524, 240–249. <https://doi.org/10.1016/j.palaeo.2019.03.036>
- Peucker-Ehrenbrink, B., & Blum, J. D. (1998). Re-Os isotope systematics and weathering of Precambrian crustal rocks: Implications for the marine osmium isotope record. *Geochimica et Cosmochimica Acta*, 62(19–20), 3193–3203. [https://doi.org/10.1016/S0016-7037\(98\)00227-0](https://doi.org/10.1016/S0016-7037(98)00227-0)
- Peucker-Ehrenbrink, B., & Jahn, B. (2001). Rhenium–osmium isotope systematics and platinum group element concentrations: Loess and the upper continental crust. *Geochemistry, Geophysics, Geosystems*, 2(10), 2001GC000172. <https://doi.org/10.1029/2001GC000172>
- Pierson-Wickmann, A. C., Reisberg, L., & France-Lanord, C. (2000). The Os isotopic composition of Himalayan river bedloads and bedrocks: Importance of black shales. *Earth and Planetary Science Letters*, 176(2), 203–218. [https://doi.org/10.1016/S0012-821X\(00\)00003-0](https://doi.org/10.1016/S0012-821X(00)00003-0)
- Poirier, A., & Gariépy, C. (2005). Isotopic Signature and Impact of Car Catalysts on the Anthropogenic Osmium Budget. *Environmental Science & Technology*, 39(12), 4431–4434. <https://doi.org/10.1021/es0484552>
- Prasad, A. K., Yang, K.-H. S., El-Askary, H. M., & Kafatos, M. (2009). Melting of major Glaciers in the western Himalayas: Evidence of climatic changes from long term MSU derived tropospheric temperature trend (1979–2008). *Annales Geophysicae*, 27(12), 4505–4519. <https://doi.org/10.5194/angeo-27-4505-2009>
- Ran, L., Lin, W. L., Deji, Y. Z., La, B., Tsering, P. M., Xu, X. B., & Wang, W. (2014). Surface gas pollutants in Lhasa, a highland city of Tibet – Current levels and pollution implications. *Atmospheric Chemistry and Physics*, 14(19), 10721–10730. <https://doi.org/10.5194/acp-14-10721-2014>
- Rauch, S., Hemond, H. F., Peucker-Ehrenbrink, B., Ek, K. H., & Morrison, G. M. (2005). Platinum Group Element Concentrations and Osmium Isotopic Composition in Urban Airborne Particles from Boston, Massachusetts. *Environmental Science & Technology*, 39(24), 9464–9470. <https://doi.org/10.1021/es051310q>
- Rodushkin, I., Engström, E., Sörlin, D., Pontér, C., & Baxter, D. C. (2007). Osmium in environmental samples from Northeast Sweden. Part II. Identification of anthropogenic sources. *The Science of the Total Environment*, 386(1–3), 159–168. <https://doi.org/10.1016/j.scitotenv.2007.06.012>
- Rupakheti, D., Adhikary, B., Praveen, P. S., Rupakheti, M., Kang, S., Mahata, K. S., et al. (2017). Pre-monsoon air quality over Lumbini, a world heritage site along the Himalayan foothills. *Atmospheric Chemistry and Physics*, 17(18), 11041–11063. <https://doi.org/10.5194/acp-17-11041-2017>
- Rupakheti, D., Kang, S., Rupakheti, M., Tripathi, L., Zhang, Q., Chen, P., & Yin, X. (2018). Long-term trends in the total columns of ozone and its precursor gases derived from satellite measurements during 2004–2015 over three different regions in South Asia: Indo-Gangetic Plain, Himalayas and Tibetan Plateau. *International Journal of Remote Sensing*, 39(21), 7384–7404. <https://doi.org/10.1080/01431161.2018.1470699>
- Saikawa, E., Panday, A., Kang, S., Gautam, R., Zusman, E., Cong, Z., et al. (2019). In P. Wester, A. Mishra, A. Mukherji, & A. B. Shrestha (Eds.), *The Hindu Kush Himalaya assessment*. Cham: Springer International Publishing. <https://doi.org/10.1007/978-3-319-92288-1>
- Schmitz, B., Peucker-Ehrenbrink, B., Lindström, M., & Tassinari, M. (1997). Accretion Rates of Meteorites and Cosmic Dust in the Early Ordovician. *Science*, 278(5335), 88–90. <https://doi.org/10.1126/science.278.5335.88>
- Selby, D., & Creaser, R. A. (2003). Re–Os geochronology of organic rich sediments: An evaluation of organic matter analysis methods. *Chemical Geology*, 200(3–4), 225–240. [https://doi.org/10.1016/S0009-2541\(03\)00199-2](https://doi.org/10.1016/S0009-2541(03)00199-2)
- Selby, D., Creaser, R. A., & Fowler, M. G. (2007). Re–Os elemental and isotopic systematics in crude oils. *Geochimica et Cosmochimica Acta*, 71(2), 378–386. <https://doi.org/10.1016/j.gca.2006.09.005>
- Selby, D., Mutterlose, J., & Condon, D. J. (2009). U–Pb and Re–Os geochronology of the Aptian/Albian and Cenomanian/Turonian stage boundaries: Implications for timescale calibration, osmium isotope seawater composition and Re–Os systematics in organic-rich sediments. *Chemical Geology*, 265(3–4), 394–409. <https://doi.org/10.1016/j.chemgeo.2009.05.005>
- Sen, I. S., Peucker-Ehrenbrink, B., & Geboy, N. (2013). Complex anthropogenic sources of platinum group elements in aerosols on Cape Cod, USA. *Environmental Science & Technology*, 47(18), 10188–10196. <https://doi.org/10.1021/es4016348>
- Sharp, M., Tranter, M., Brown, G. H., & Skidmore, M. (1995). Rates of chemical denudation and CO drawdown in a glacier-covered alpine catchment. *Geology*, 23(1), 61. [https://doi.org/10.1130/0091-7613\(1995\)023<0061:ROCDAC>2.3.CO;2](https://doi.org/10.1130/0091-7613(1995)023<0061:ROCDAC>2.3.CO;2)

- Shrestha, P., Barros, A. P., & Khlystov, A. (2010). Chemical composition and aerosol size distribution of the middle mountain range in the Nepal Himalayas during the 2009 pre-monsoon season. *Atmospheric Chemistry and Physics*, 10(23), 11605–11621. <https://doi.org/10.5194/acp-10-11605-2010>
- Singh, P., Sarawade, P., & Adhikary, B. (2020). Transport of black carbon from planetary boundary layer to free troposphere during the summer monsoon over South Asia. *Atmospheric Research*, 235, 104761. <https://doi.org/10.1016/j.atmosres.2019.104761>
- Singh, S. K., Trivedi, J. R., & Krishnaswami, S. (1999). Re-Os isotope systematics in black shales from the Lesser Himalaya: Their chronology and role in the 187Os/188Os evolution of seawater. *Geochimica et Cosmochimica Acta*, 63(16), 2381–2392. [https://doi.org/10.1016/S0016-7037\(99\)00201-X](https://doi.org/10.1016/S0016-7037(99)00201-X)
- Singh, S. M., Sharma, J., Gawas-Sakhalkar, P., Upadhyay, A. K., Naik, S., Pedneker, S. M., & Ravindra, R. (2013). Atmospheric deposition studies of heavy metals in Arctic by comparative analysis of lichens and cryoconite. *Environmental Monitoring and Assessment*, 185(2), 1367–1376. <https://doi.org/10.1007/s10661-012-2638-5>
- Sproson, A. D., Selby, D., Suzuki, K., Oda, T., & Kuroda, J. (2020). Anthropogenic Osmium in Macroalgae from Tokyo Bay Reveals Widespread Contamination from Municipal Solid Waste. *Environmental Science & Technology*, 54(15), 9356–9365. <https://doi.org/10.1021/acs.est.0c01602>
- Stockwell, C. E., Christian, T. J., Goetz, J. D., Jayarathne, T., Bhave, P. V., Praveen, P. S., et al. (2016). Nepal Ambient Monitoring and Source Testing Experiment (NAMASte): Emissions of trace gases and light-absorbing carbon from wood and dung cooking fires, garbage and crop residue burning, brick kilns, and other sources. *Atmospheric Chemistry and Physics*, 16(17), 11043–11081. <https://doi.org/10.5194/acp-16-11043-2016>
- Thakur, S. S., & Patel, S. C. (2012). Mafic and pelitic xenoliths in the Kinnaur Kailash Granite, Baspa river valley, NW Himalaya: Evidence of pre-Himalayan granulite metamorphism followed by cooling event. *Journal of Asian Earth Sciences*, 56, 105–117. <https://doi.org/10.1016/j.jseae.2012.04.024>
- Thöni, M., Miller, C., Hager, C., Grasemann, B., & Horschneegg, M. (2012). New geochronological constraints on the thermal and exhumation history of the Lesser and Higher Himalayan Crystalline Units in the Kullu–Kinnaur area of Himachal Pradesh (India). *Journal of Asian Earth Sciences*, 52, 98–116. <https://doi.org/10.1016/j.jseae.2012.02.015>
- Thorpe, M. T., Hurowitz, J. A., & Dehouck, E. (2019). Sediment geochemistry and mineralogy from a glacial terrain river system in southwest Iceland. *Geochimica et Cosmochimica Acta*, 263, 140–166. <https://doi.org/10.1016/j.gca.2019.08.003>
- Tranter, M., Sharp, M. J., Lamb, H. R., Brown, G. H., Hubbard, B. P., & Willis, I. C. (2002). Geochemical weathering at the bed of Haut Glacier d'Arolla, Switzerland: A new model. *Hydrological Processes*, 16(5), 959–993. <https://doi.org/10.1002/hyp.309>
- van Acken, D., Tütken, T., Daly, J. S., Schmid-Röhl, A., & Orr, P. J. (2019). Rhenium-osmium geochronology of the Toarcian Posidonia Shale, SW Germany. *Palaeogeography, Palaeoclimatology, Palaeoecology*, 534, 109294. <https://doi.org/10.1016/j.palaeo.2019.109294>
- Wake, C. P., Mayewski, P. A., Zichu, X., Ping, W., & Zhongqin, L. (1993). Regional distribution of monsoon and desert dust signals recorded in Asian glaciers. *Geophysical Research Letters*, 20(14), 1411–1414. <https://doi.org/10.1029/93GL01682>
- Walker, R., Horan, M., Morgan, J., Becker, H., Grossman, J., & Rubin, A. (2002). Comparative ¹⁸⁷Re–¹⁸⁷Os systematics of chondrites. *Geochimica et Cosmochimica Acta*, 66(23), 4187–4201. [https://doi.org/10.1016/S0016-7037\(02\)01003-7](https://doi.org/10.1016/S0016-7037(02)01003-7)
- Xu, B., Cao, J., Hansen, J., Yao, T., Joswia, D. R., Wang, N., et al. (2009). Black soot and the survival of Tibetan glaciers. *Proceedings of the National Academy of Sciences*, 106(52), 22114–22118. <https://doi.org/10.1073/pnas.0910444106>
- Yan, F., He, C., Kang, S., Chen, P., Hu, Z., Han, X., et al. (2019). Deposition of Organic and Black Carbon: Direct Measurements at Three Remote Stations in the Himalayas and Tibetan Plateau. *Journal of Geophysical Research: Atmospheres*, 124(16), 9702–9715. <https://doi.org/10.1029/2019JD031018>
- Yarragunta, Y., Srivastava, S., Mitra, D., & Chandola, H. C. (2020). Influence of forest fire episodes on the distribution of gaseous air pollutants over Uttarakhand, India. *GIScience and Remote Sensing*, 57(2), 190–206. <https://doi.org/10.1080/15481603.2020.1712100>
- Yudovskaya, M. A., Tessalina, S., Distler, V. V., Chaplygin, I. V., Chugaev, A. V., & Dikov, Y. P. (2008). Behavior of highly siderophile elements during magma degassing: A case study at the Kudryavy volcano. *Chemical Geology*, 248(3–4), 318–341. <https://doi.org/10.1016/j.chemgeo.2007.12.008>
- Zhang, Q., Kang, S., Kaspari, S., Li, C., Qin, D., Mayewski, P. A., & Hou, S. (2009). Rare earth elements in an ice core from Mt. Everest: Seasonal variations and potential sources. *Atmospheric Research*, 94(2), 300–312. <https://doi.org/10.1016/j.atmosres.2009.06.005>

References From the Supporting Information

- Agarwal, A. K., Singh, A. P., Gupta, T., Agarwal, R. A., Sharma, N., Rajput, P., et al. (2018). Mutagenicity and cytotoxicity of particulate matter emitted from biodiesel-fueled engines. *Environmental Science & Technology*, 52(24), 14496–14507. research-article. <https://doi.org/10.1021/acs.est.8b03345>
- Alizai, A., Carter, A., Clift, P. D., VanLaningham, S., Williams, J. C., & Kumar, R. (2011). Sediment provenance, reworking and transport processes in the Indus River by U–Pb dating of detrital zircon grains. *Global and Planetary Change*, 76(1–2), 33–55. <https://doi.org/10.1016/j.gloplacha.2010.11.008>
- Barbieri, M. (2016). The importance of enrichment factor (EF) and geoaccumulation index (Igeo) to evaluate the soil contamination. *Journal of Geology and Geophysics*, 5(1), 1000237. <https://doi.org/10.4172/2381-8719.1000237>
- Brun, F., Wagnon, P., Berthier, E., Jomelli, V., Maharjan, S. B., Shrestha, F., & Kraaijenbrink, P. D. A. (2019). Heterogeneous influence of glacier morphology on the mass balance variability in high mountain Asia. *Journal of Geophysical Research: Earth Surface*, 124(6), 1331–1345. <https://doi.org/10.1029/2018JF004838>
- Castillo, S., Moreno, T., Querol, X., Alastuey, A., Cuevas, E., Herrmann, L., et al. (2008). Trace element variation in size-fractionated African desert dusts. *Journal of Arid Environments*, 72(6), 1034–1045. <https://doi.org/10.1016/j.jaridenv.2007.12.007>
- Chang, Q., Mishima, T., Yabuki, S., Takahashi, Y., & Shimizu, H. (2000). Sr and Nd isotope ratios and REE abundances of moraines in the mountain areas surrounding the Taklimakan Desert, NW China. *Geochemical Journal*, 34(6), 407–427. <https://doi.org/10.2343/geochemj.34.407>
- Cogley, J. G. (2012). Himalayan glaciers in the balance. *Nature*, 488(7412), 468–469. <https://doi.org/10.1038/488468a>
- Das, B. K., & Haake, B. G. (2003). Geochemistry of Rewalsar Lake sediment, Lesser Himalaya, India: Implications for source-area weathering, provenance and tectonic setting. *Geosciences Journal*, 7(4), 299–312. <https://doi.org/10.1007/BF02919560>
- Ferrat, M., Weiss, D. J., Strekopytov, S., Dong, S., Chen, H., Najorka, J., et al. (2011). Improved provenance tracing of Asian dust sources using rare earth elements and selected trace elements for palaeomonsoon studies on the eastern Tibetan Plateau. *Geochimica et Cosmochimica Acta*, 75(21), 6374–6399. <https://doi.org/10.1016/j.gca.2011.08.025>

- Islam, R., Ghosh, S. K., Vyshnavi, S., & Sundariyal, Y. P. (2011). Petrography, geochemistry and regional significance of crystalline klippen in the Garhwal Lesser Himalaya, India. *Journal of Earth System Science*, 120(3), 489–501. <https://doi.org/10.1007/s12040-011-0086-1>
- Li, D., Ma, B., Jiang, F., & Wang, P. (2011). Nature, genesis and provenance of silt pellets on the ice surface of Glacier No. 1, upper Urumqi River, Tian Shan, Northwestern China. *Quaternary International*, 236(1–2), 107–115. <https://doi.org/10.1016/j.quaint.2010.10.004>
- Maibam, B., Singh, Y. R., Shukla, A. D., & Ramanathan, A. L. (2016). Geochemical study of the granitoids around Chhota Shigri. *Journal of Applied Geochemistry*, 18(4), 408–413.
- McLennan, S. M. (1993). Weathering and global denudation. *The Journal of Geology*, 101(2), 295–303. <https://doi.org/10.1086/648222>
- Miller, C., Thoni, M., Frank, W., Grasemann, B., Klotzli, U., Guntli, P., & Draganits, E. (2001). The early Palaeozoic magmatic event in the Northwest Himalaya, India: Source, tectonic setting and age of emplacement. *Geological Magazine*, 138(3), 237–251. <https://doi.org/10.1017/S0016756801005283>
- Panwar, S., Agarwal, V., & Chakrapani, G. J. (2017). Morphometric and sediment source characterization of the Alaknanda river basin, headwaters of river Ganga, India. *Natural Hazards*, 87(3), 1649–1671. <https://doi.org/10.1007/s11069-017-2838-y>
- Parsons, A. J., & Abrahams, A. D. (2009). Geomorphology of desert environments. In A. J. Parsons, & A. D. Abrahams (Eds.), *Geomorphology of desert environments*. Geomorphology of desert environments. Dordrecht: Springer Netherlands. <https://doi.org/10.1007/978-1-4020-5719-9>
- Pye, K. (1995). The nature, origin and accumulation of loess. *Quaternary Science Reviews*, 14(7–8), 653–667. [https://doi.org/10.1016/0277-3791\(95\)00047-X](https://doi.org/10.1016/0277-3791(95)00047-X)
- Ramsankaran, R., Pandit, A., & Azam, M. F. (2018). Spatially distributed ice-thickness modelling for Chhota Shigri Glacier in western Himalayas, India. *International Journal of Remote Sensing*, 39(10), 3320–3343. <https://doi.org/10.1080/01431161.2018.1441563>
- Ranjan, N., & Banerjee, D. M. (2009). Central Himalayan crystallines as the primary source for the sandstone–mudstone suites of the Siwalik Group: New geochemical evidence. *Gondwana Research*, 16(3–4), 687–696. <https://doi.org/10.1016/j.gr.2009.07.005>
- Richards, A., Argles, T., Harris, N., Parrish, R., Ahmad, T., Darbyshire, F., & Draganits, E. (2005). Himalayan architecture constrained by isotopic tracers from clastic sediments. *Earth and Planetary Science Letters*, 236(3–4), 773–796. <https://doi.org/10.1016/j.epsl.2005.05.034>
- Roy, P. D., & Smykatz-Kloss, W. (2007). REE geochemistry of the recent playa sediments from the Thar Desert, India: An implication to playa sediment provenance. *Geochemistry*, 67(1), 55–68. <https://doi.org/10.1016/j.chemer.2005.01.006>
- Rudnick, R. L., & Gao, S. (2014). Composition of the continental crust. In K. K. T. H. D. Holland (Ed.), *Treatise on geochemistry* (2nd ed., pp. 1–51). Elsevier. <https://doi.org/10.1016/B978-0-08-095975-7.00301-6>
- Shao, Y. (2009). Physics and modelling of wind erosion. In Y. Shao (Ed.), *Physics and modelling of wind erosion*. Berlin Heidelberg, Dordrecht: Springer-VerlagSpringer Netherlands. <https://doi.org/10.1007/978-1-4020-8895-7>
- Srivastava, R. K., & Sahai, A. (2001). High-field strength element geochemistry of mafic intrusive rocks from the Bhagirathi and Yamuna Valleys, Garhwal Himalaya, India. *Gondwana Research*, 4(3), 455–463. [https://doi.org/10.1016/S1342-937X\(05\)70345-2](https://doi.org/10.1016/S1342-937X(05)70345-2)
- Srivastava, R. K., & Samal, A. K. (2019). Geochemical characterization, petrogenesis, and emplacement tectonics of Paleoproterozoic high-Ti and low-Ti mafic intrusive rocks from the western Arunachal Himalaya, northeastern India and their possible relation to the ~1.9 Ga LIP event of the Indian s. *Geological Journal*, 54(1), 245–265. <https://doi.org/10.1002/gj.3172>
- Taylor, S. R., & McLennan, S. M. (1985). *The continental crust: Its composition and evolution*. Malden, Mass: Blackwell.
- Vincent, C., Ramanathan, A., Wagnon, P., Dobhal, D. P., Linda, A., Berthier, E., et al. (2013). Balanced conditions or slight mass gain of glaciers in the Lahaul and Spiti region (northern India, Himalaya) during the nineties preceded recent mass loss. *The Cryosphere*, 7(2), 569–582. <https://doi.org/10.5194/tc-7-569-2013>
- Wagnon, P., Linda, A., Arnaud, Y., Kumar, R., Sharma, P., Vincent, C., et al. (2007). Four years of mass balance on Chhota Shigri Glacier, Himachal Pradesh, India, a new benchmark glacier in the western Himalaya. *Journal of Glaciology*, 53(183), 603–611. <https://doi.org/10.3189/002214307784409306>